

Chapter 1

Introduction

Titanium alloys have excellent properties such as high melting point (1820°C), high strength, low density (4.5 gm/cm³), good creep resistance up to about 550°C, and excellent corrosion resistance to consider for many applications, including aircraft, aero-engines, biomedical devices (high strength and corrosion resistance), and components in the chemical processing equipment.

1.1 Titanium and its Alloys

1.1.1 Crystal Structure of Titanium

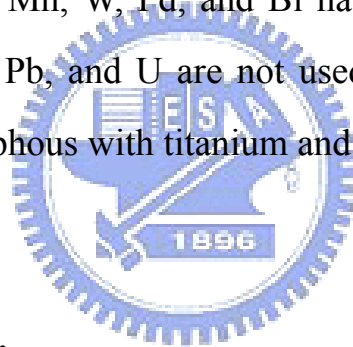
Pure titanium exhibits an allotropic phase transformation at 882°C. Above 882°C, titanium is body-centered cubic (bcc) β phase and below this temperature it is hexagonal close-packed crystal structure (α phase). The c/a ratio for pure α titanium is 1.587. The hexagonal unit cell of the α phase is shown in Fig. 1.1, also indicating the room temperature values of the lattice parameters with $a \approx 0.295$ nm and $c \approx 0.468$ nm.¹ The unit cell of the body centered cubic (bcc) β phase is illustrated in Fig. 1.2, indicating the lattice parameter value ($a \approx 0.332$ nm) of pure β titanium at 900°C.¹

1.1.2 Phase Diagram

Alloying elements additions in titanium are usually classified into α or β stabilizer, depending on whether they increase or decrease the transformation

temperature of α/β of pure titanium. Figure 1.3. displays that the interstitial elements O, N, and C are all effective α stabilizers and increase the transformation temperature of β to α .²

The common β stabilizing elements are divided into two types: β isomorphous and β eutectoid. Both types of phase diagrams are shown schematically in Fig. 1.3.² These β isomorphous elements (V, Mo, and Nb) make likely to stabilize the β phase in titanium to room temperature. Ta and Re belong to this group but there are rarely used or not used at all. In the β eutectoid elements, the Cr, Fe, and Si are used in many titanium alloys. Additionally, the Ni, Cu, Mn, W, Pd, and Bi have only very limited usage and Co, Ag, Au, Pt, Be, Pb, and U are not used at all in titanium alloys.² The element Zr is isomorphous with titanium and completely soluble in the α and β phases of titanium.



1.1.3 Casting of Titanium

The high reactivity of titanium with oxygen limits the maximum use temperature of titanium alloys to about 600°C. Above this temperature the diffusion of oxygen through the oxide surface layer becomes too fast and results in excessive growth of the oxide layer and embitterment of the adjacent oxygen rich layer of the titanium alloy. Therefore, special means are required to produce ingots of both unalloyed titanium (CP titanium) and the various titanium alloys.

Titanium is often melted in a water-cooled copper crucible by consumable electrode vacuum arc melting instead of vacuum induction melting (VIM)

because ceramic crucibles, used in the VIM process, can react with the titanium melt. Therefore, how to control the interfacial reactions between titanium and ceramics is of great concern.

Titanium and its alloys are melted either in a vacuum arc remelt (VAR) furnace or in a cold hearth melting (CHM) furnace. Titanium Castings are produced by vacuum arc remelting in a copper water-cooled crucible. A schematic diagram of a vacuum casting furnace for titanium alloys is shown in Fig. 1.4.³ The high reactivity of titanium requires the use of a non-reactive melting technique. The methods available include non-consumable electrode and consumable electrode VAR and cold walled split crucible induction melting.

1.2 Y_2O_3 - ZrO_2

1.2.1 Phase Diagram



Y_2O_3 is an effective solute for stabilizing the cubic and tetragonal forms of ZrO_2 and increasing the thermal and mechanical properties of ZrO_2 .⁴ At the temperatures ranging from 500° to 1000°C, approximately 1.5 mol% Y_2O_3 is soluble in *t*- ZrO_2 and can fully stabilize it into *c*- ZrO_2 about approximately 7.5 mol%.⁵ A two-phase region of *t*- and *c*- ZrO_2 exists in between 1.5 to 7.5 mol% Y_2O_3 . The binary ZrO_2 - Y_2O_3 phase diagram is shown in Fig. 1.5.⁵

1.2.2 The $c \rightarrow t$ -ZrO₂ Diffusion Transformation

It is well known that $c \rightarrow t$ phase transformation of zirconia can be by a diffusional or diffusionless process.⁶ During cooling, a given alloy within composition in the $c + t$ two phase field, the precipitation of the t -ZrO₂ and simultaneously the c -ZrO₂ with high Y₂O₃ is expected. The precipitation reaction to form t -ZrO₂ by a diffusional process requires extensive local compositional changes, and relatively long annealing periods are needed to achieve phase equilibrium.

The $c \rightarrow t$ -ZrO₂ by the diffusional phase transformation in the binary partially stabilized zirconia (PSZ) system has been extensively studied.⁷⁻¹¹ The early stage of the precipitation of t -ZrO₂ in PSZ (Y₂O₃-PSZ) causes a tweed-like contrast and high coherency strains which will lead to strain-induced coarsening during annealing.^{9, 12} The twinned t -ZrO₂ precipitates (or colonies) among the c -ZrO₂ matrix were found after long-term annealing at 1400° to 1600°C.^{9, 10} This aging for about 100 h allowed the formation and growth of low-solute t -ZrO₂ precipitates in high-solute cubic solid solution matrix.^{7, 10} The t -ZrO₂ with colonies morphology had internally twinned microstructure which the c axes of two twin-related variants are not at 90° but at 89°.¹¹ These t -ZrO₂ colonies can coarsen and do not readily transform to m -ZrO₂ even when they become quite large.⁷ Nevertheless, they are metastable at room temperature and may undergo the stress-induced martensitic transformation.¹³

1.2.3 The $c \rightarrow t'$ -ZrO₂ Diffusionless Transformation

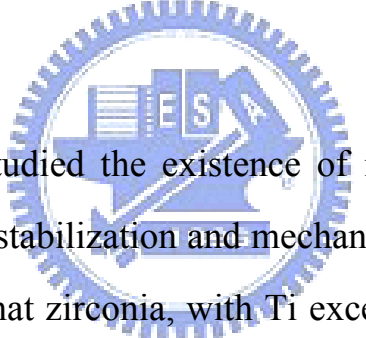
If the annealing is rapidly cooled from a high temperature so as to avoid any

diffusion-controlled transformation, the system can decrease its overall free energy only by transforming to some metastable, referred to as t' phase, via a diffusionless transformation.¹³ Depending on the cooling rate, the precipitation via a diffusional transformation is a process competitive with the diffusionless (displacive) $c \rightarrow t'$ -ZrO₂ transformation.¹³ If the cooling rate is very slow, nucleation and limited growth of the t -ZrO₂ precipitates can occur. If these alloys are rapidly cooled from the single phase c field, the c -ZrO₂ phase undergoes a displacive and diffusionless phase transformation to t symmetry. This first recognized by Lefevre¹⁴ and studied in a comprehensive manner by Scott,¹⁵ who showed that this transformation could occur in alloys containing from ~ 6 to ~ 13 wt% Y₂O₃. Later the workers¹⁶ who found this high-Y₂O₃ phase in plasma-sprayed materials called this phase “non-transformable” t' -ZrO₂, because of its reluctance to undergo the martensitic transformation to monoclinic (m -ZrO₂) symmetry.

The microstructures of the t' -ZrO₂ are characterized by the presence of anti-phase domain boundaries (APB's) because of the reduction in symmetry during the phase transformation. The transformation may also be accompanied by the mechanical deformation of twins. The twinned t' -ZrO₂ phase, which resulted from the untransformable t' -ZrO₂, were featured by a high Y₂O₃ content up to 10 wt% as mentioned in several other previous studies.⁶ The twins were able to relieve the strains arising from the small tetragonality of the product phase and the small molar volume change accompanying transformation.⁶

1.3 Ti/ZrO₂ System

The reactions between titanium and zirconia have been subjected to an intensive investigation, indicating that zirconia became oxygen-deficient because of the interfacial reaction. Economos and Kingery¹⁷ revealed that titanium penetrated along the grain boundaries of ZrO₂ with the formation of the oxygen-deficient zirconia. Ruh¹⁸ reported that up to 4 at.% of titanium was retained in zirconia at room temperature, while up to approximately 10 mol% zirconia would be dissolved in titanium. Zirconium entered into the titanium lattice substitutionally and oxygen entering interstitial positions, but no evidence of other compounds except oxygen-deficient zirconia at the interface was provided.



Some researchers have studied the existence of interfacial phases and the effects of titanium on the stabilization and mechanical properties of zirconia. Weber *et al.*¹⁹ indicated that zirconia, with Ti exceeding the solubility limit, showed good strength and thermal shock resistance. Lin *et al.*²⁰ stated that zirconia was stabilized because of the dissolution of TiO, formed by the reaction between titanium and residual trace oxygen in the vacuum furnace. The improvement in the strength and the thermal shock resistance of zirconia was attributed to the dissolution of TiO as well.

According to the pseudobinary diagram of Ti-ZrO₂ proposed by Domagala *et al.*,²¹ (Ti, Zr)₃O could precipitate from the supersaturated solid solution of α -Ti(Zr, O) during cooling. However, Weber *et al.*¹⁹ and Lin *et al.*²⁰ found neither (Ti, Zr)₃O nor α -Ti (Zr, O). Recently, Zhu *et al.*²² investigated the

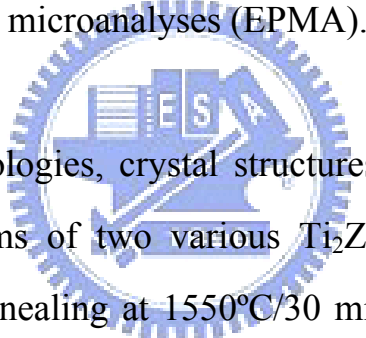
wettability and the interaction between pure liquid titanium and yttria-stabilized zirconia by sessile drop method in Ar atmosphere at 1700°C. They found that there existed two distinct chemical reaction layers in the interface but not identified.

Lin and his coworkers²³⁻²⁶ have investigated on the diffusional reaction between titanium and zirconia. Using TEM/EDS analyses, they indicated that an ordered titanium suboxide (Ti_3O) and the orthorhombic lamellae Ti_2ZrO were formed in the solid solution of α -Ti(O) during cooling from 1700°C. In addition to the lamellar Ti_2ZrO and α -Ti(O), the orthorhombic β' -Ti(Zr, O) and an spherical ordered Ti_2ZrO phase were also found in the metal side after annealing at 1550°C.²⁴ The orientation relations between the α -Ti (Zr, O) and lamellae Ti_2ZrO were determined to be $[0001]_{\alpha-Ti} // [110]_{Ti_2ZrO}$ and $(10\bar{1}0)_{\alpha-Ti} // (1\bar{1}0)_{Ti_2ZrO}$; meanwhile those between the α -Ti and the spherical ordered Ti_2ZrO were $[0001]_{\alpha-Ti} // [0001]_{Ti_2ZrO}$ and $(10\bar{1}0)_{\alpha-Ti} // (10\bar{1}0)_{Ti_2ZrO}$. Furthermore, the acicular α -Ti was precipitated in the β' -Ti matrix with two various orientation relations in the metal side.²⁵ One of the orientation relations was determined to be $[2\bar{1}\bar{1}0]_{\alpha-Ti} // [001]_{\beta'-Ti}$ and $(0001)_{\alpha-Ti} // (100)_{\beta'-Ti}$ and the other was $[2\bar{1}\bar{1}0]_{\alpha-Ti} // [021]_{\beta'-Ti}$ and $(0001)_{\alpha-Ti} // (1\bar{1}2)_{\beta'-Ti}$.²⁵ It is focusing upon the microstructure of zirconia side far away from the interface of Ti/ZrO₂, Lin and Lin²⁶ also observed twinned t' -ZrO_{2-x}, lenticular t -ZrO_{2-x}, and/or ordered c -ZrO_{2-x} as well as the intergranular α -Zr after reaction at 1550°C.

1.4 Thesis Outline

Chapter 1 describes the basic applications and principles of titanium and zirconia about their structures, casting of titanium, and phase diagrams. It also reviews the recent literature talking about titanium and zirconia reaction.

In this study, the interfaces of titanium and zirconia after annealing at various temperatures and periods were characterized using analytical scanning electron microscopy (SEM), analytical transmission electron microscopy (TEM), both attached with an energy-dispersive spectrometer (EDS), and electron probe microanalyses (EPMA).



In Chapter 2, the morphologies, crystal structures, chemical compositions, and formation mechanisms of two various Ti_2ZrO phases formed in the Ti/ ZrO_2 interface after annealing at $1550^\circ\text{C}/30$ min will be explored. The lamellar and the spherical Ti_2ZrO as well as the orthorhombic β' -Ti were first found to exist in the titanium side after cooling down to room temperature. The orientation relations between α -Ti and Ti_2ZrO were determined using stereographic projection analyses.

Chapter 3 will intensively investigate the phases and microstructure in the ceramic side of the Ti/ ZrO_2 diffusion couple isothermally annealed at temperatures ranging from 1100° to 1550°C . Three distinct microstructures were found in the ceramic side away from the interface of Ti/ ZrO_2 , depending upon the annealing temperature. We will delve into the

microstructural evolution in zirconia side at various annealing temperatures.

In Chapter 4, the diffusional reaction between titanium and zirconia will be carried out at 1550°C for 0.5, 3, and 6 h. The distinct reaction layers in the reaction affected zone between Ti and ZrO₂ were investigated. Using the Ti-Zr-O phase diagram, the microstructural evolution and formation mechanisms of the reaction layers between titanium and zirconia isothermally annealed at 1550°C was attempted to be proposed.

Chapter 5 will further discuss the titanium and zirconia diffusion couples isothermally annealed in argon at temperatures between 1100° to 1550°C. It was found that the microstructure in the Ti/ZrO₂ interface strongly depended upon the temperature so that very distinct reaction layers were developed at various temperatures. The microstructural developments and the diffusion paths in the Ti/ZrO₂ diffusion couples annealed for various temperatures will be described by the aid of the Ti-Zr-O ternary phase diagram.

Finally, microstructural characterization, evolution, and formation mechanisms of the various reaction layers between titanium and zirconia at various annealing temperatures between 1100° and 1550°C will be summarized in Chapter 6.

Reference

1. G. Lutjering and J. C. Williams *Titanium*; Springer-Verlag, Berlin, Germany, Ch. 5, p. 14, 2003.

2. G. Lutjering and J. C. Williams *Titanium*; Springer-Verlag, Berlin, Germany, Ch. 5, p. 22, 2003.
3. G. Lutjering and J. C. Williams *Titanium*; Springer-Verlag, Berlin, Germany, Ch. 5, p. 88, 2003.
4. K. Tsukuma, Y. Kubota, and T. Tsukidate, "Thermal and Mechanical Properties of Y₂O₃-stabilized Tetragonal Zirconia Polycrystals," pp. 382-390 in *Advances in Ceramics, Vol. 12, Science and Technology of Zirconia II*. Edited by N. Claussen, M. Rühle, and A. H. Heuer, American Ceramic Society, Columbus, OH, 1984
5. R. Ruh, K. S. Mazdiyashni, P. G. Valentine, and H. O. Bielstein, "Phase Relations in the System ZrO₂-Y₂O₃ at Low Y₂O₃ Contents," *J. Am. Ceram. Soc.*, **67**[9], c-190-192 (1984).
6. A. H. Heuer, "The Displacive Cubic → Tetragonal Transformation in ZrO₂ Alloys," *Acta metall.*, **35**[3], 661-666 (1987).
7. V. Lanteri, A. H. Heuer, and T. E. Mitchell, "Tetragonal Phase in the System ZrO₂ - Y₂O₃," pp.118-130 in *Advances in Ceramics, Vol. 12, Science and Technology of Zirconia II*. Edited by N. Claussen, M. Rühle, and A. H. Heuer, American Ceramic Society, Columbus, OH, 1984
8. A. H. Heuer and M. Rühle, "Phase Transformations in ZrO₂-Containing Ceramic: I, the Instability of c-ZrO₂ and the Resulting Diffusion-Controlled Reactions," pp. 1-13 in *Advances in Ceramics, Vol. 12, Science and Technology of Zirconia II*. Edited by N. Claussen, M. Rühle, and A. H. Heuer, American Ceramic Society, Columbus, OH, 1984
9. R. Chaim, M. Rühle, and A. H. Heuer, "Microstructural Evolution in a ZrO₂-12 Wt% Y₂O₃ Ceramic," *J. Am. Ceram. Soc.*, **68**[8], 27-31 (1985).
10. A. H. Heuer, V. Lanteri, and A. Dominguez-Rodriguez, "High-Temperature Precipitation Hardening of Y₂O₃ Partially-Stabilized

- ZrO₂ (Y-PSZ) Single Crystals," *Acta metall.*, **37**[2], 559-67 (1989).
11. N. Ishizawa, A. Saiki, T. Yagi, N. Mizutani, and M. Kato, "Twin-Related Tetragonal Variants in Yttria Partially Stabilized Zirconia," *J. Am. Ceram. Soc.*, **69**[2], C-18-C-20 (1985).
 12. M. Rühle, N. Claussen, and A. H. Heuer, "Microstructural Studies of Y₂O₃-Containing Tetragonal ZrO₂ Polycrystals (Y-TZP)," pp. 352-370 in *Advances in Ceramics, Vol. 12, Science and Technology of Zirconia II*. Edited by N. Claussen, M. Rühle, and A. H. Heuer, American Ceramic Society, Columbus, OH, 1984
 13. A. H. Heuer, R. Chaim, and V. Lanteri, "Review Article: Phase Transformations and Microstructural Characterization of Alloys in the System Y₂O₃-ZrO₂," pp. 3-20 in *Advances in Ceramics, Vol. 24, Science and Technology of Zirconia III*. Edited by N. Claussen, M. Rühle, and A. H. Heuer, American Ceramic Society, Columbus, OH, 1988
 14. J. Lefevre, "Study of a Discontinuous Deformation of the Fluorite Cell," *J. Ann. Chim. (Paris)*, **8**[1-2], 118-149 (1963).
 15. H. G. Scoot, "Phase Relationships in the Zirconia-Yttria System," *J. Mater. Sci.*, **10**[9], 1527-1535 (1975).
 16. A. M. Robert, L. S. James, and G. G. Ralph, "Phase Stability in Plasma-sprayed, Partially Stabilized Zirconia-Yttria," pp. 241-253 in, *Advances in Ceramics, Vol. 3, Science and Technology of Zirconia II*. Edited by N. Claussen, M. Rühle, and A. H. Heuer, American Ceramic Society, Columbus, OH, 1984
 17. G. Economos and W. D. Kingery, "Metal-Ceramic Interactions:II, Metal Oxide Interfacial Reactions at Elevated Temperatures," *J. Am. Ceram. Soc.*, **36**[12], 403-09 (1953).
 18. R. Ruh, N. M. Tallan, and H. A. Lipsitt, "Effect of Metal Additions on

- the Microstructure of Zirconia," *J. Am. Ceram. Soc.*, **47**[12], 632-35 (1964).
19. B. C. Weber, H. J. Garrett, F. A. Mauer, and M. A. Schwartz, "Observations on the Stabilization of Zirconia," *J. Am. Ceram. Soc.*, **39**[6], 197-07 (1956).
 20. C. L. Lin, D. Gan, and P. Shen, "Stabilization of Zirconia Sintered with Titanium," *J. Am. Ceram. Soc.*, **71**[8], 624-29 (1988).
 21. R. F. Domagala, S. R. Lyon, and R. Ruh, "The Pseudobinary Ti-ZrO₂," *J. Am. Ceram. Soc.*, **56**[11], 584-87 (1973).
 22. J. Zhu , A. Kamiya, T. Yamada, W. Shi, K. Naganuma, and K. Mukai, "Surface tension, Wettability and Reactivity of Molten Titanium in Ti/Yttria-Stabilized Zirconia System," *Mater. Sci. Engng. A*, **A327**, 117-27 (2002).
 23. K. F. Lin and C. C. Lin, "Transmission Electron Microscope Investigation of The Interface between Titanium and Zirconia," *J. Am. Ceram. Soc.*, **82**[11], 3179-3185 (1999).
 24. K. L. Lin and C. C. Lin, "Ti₂ZrO Phases Formed in the Titanium and Zirconia Interface after Reaction at 1550°C," *J. Am. Ceram. Soc.*, **88**[5], 1268-272 (2005).
 25. K. L. Lin and C. C. Lin, "Microstructural Evolution and Formation Mechanism of the Interface between Zirconia and Titanium Annealed at 1550°C," accepted by *J. Am. Ceram. Soc.*, (2005).
 26. K. L. Lin and C. C. Lin, "Zirconia-Related Phases in the Zirconia/Titanium Diffusion Couple after Annealing at 1100° to 1550°C " *J. Am. Ceram. Soc.*, **88**[10] 2928 – 934 (2005).

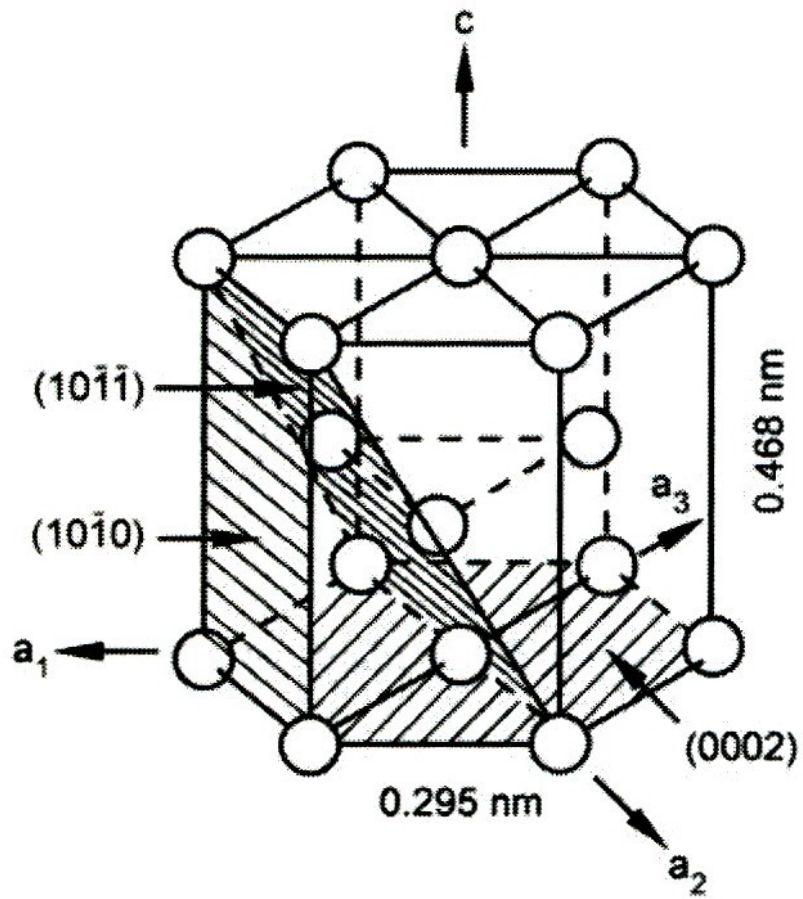


Fig. 1.1 Unit cell of α -Ti.

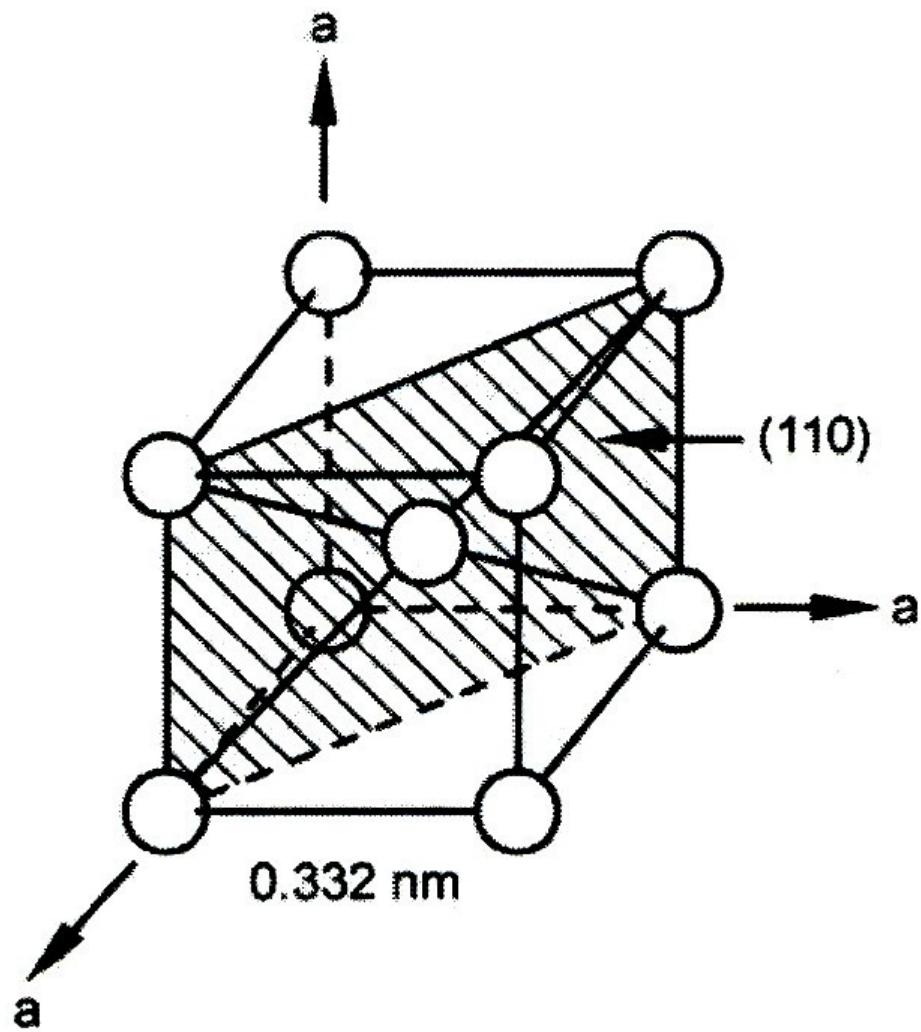


Fig. 1.2 Unit cell of β -Ti.

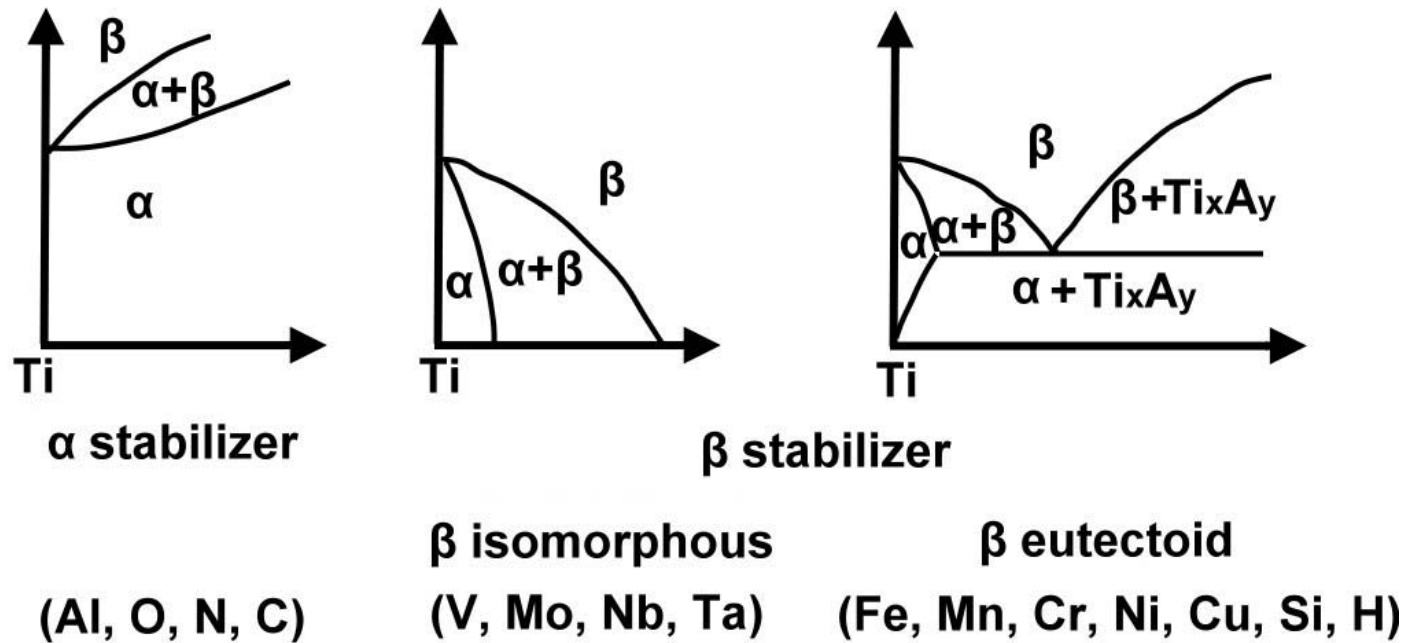


Fig. 1.3 Effect of alloying elements on phase diagrams of titanium alloys (schematically).

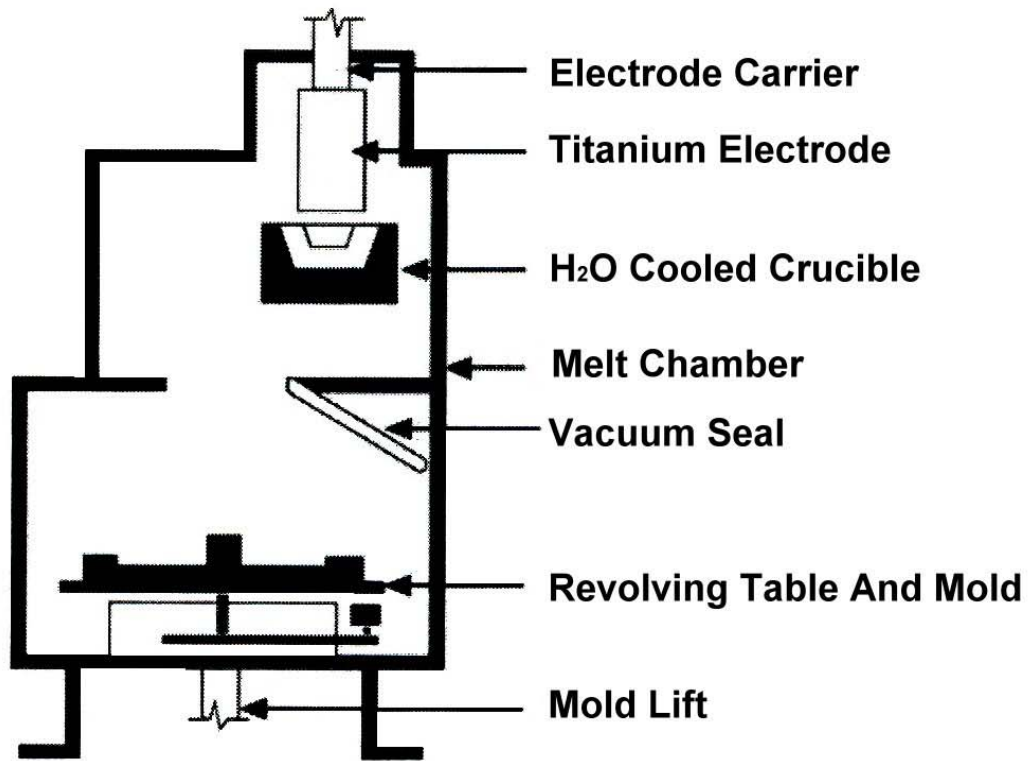


Fig. 1.4 Schematic of a vacuum casting furnace used for making titanium castings.

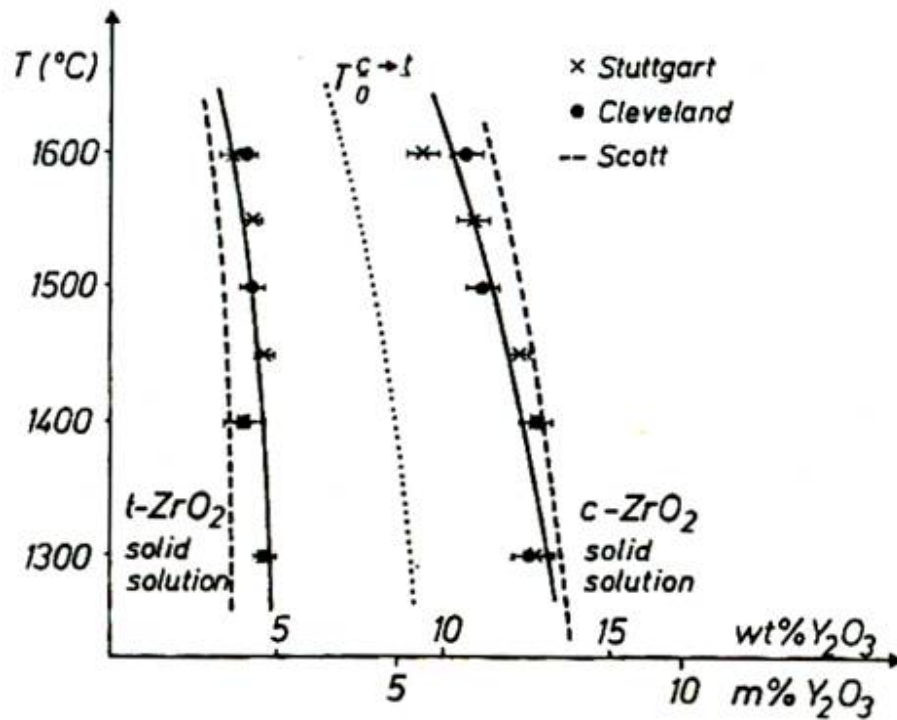


Fig. 1.5 Section of ZrO_2 -rich part of the $\text{ZrO}_2\text{-Y}_2\text{O}_3$ phase diagram. Composition limits were determined by analytical transmission electron microscopy.

